doi:10.1038/nature11259

Materials and Methods

Yeast experiment

Constructs and strains

All constructs used in this study (Supplementary Table 1) were cloned using a combinatorial cloning strategy based on the Type II restriction enzyme AarI developed by Peisajovich et al[1]. For the MAPK pathway specific inhibitory experiments, strain WP022 and WP116 were constructed from the W303-derived strain SP147 (Supplementary Table 2) by tagging the C-terminal of endogenous Pbs2 or Ste5 with leucine zipper respectively. To construct WP039 for measuring the nuclear Hog1 accumulation, the C-terminal of endogenous Hog1 in wild type W303 strain was tagged with GFP using standard integration technique. A histone protein Htb2 was C-terminally tagged with mCherry and the expression was driven by *ADH1* promoter. This Htb2-mCherry fusion protein was integrated at *TRP1* locus for the visualization of the nucleus. Endogenous Pbs2 was tagged with a leucine zipper by PCR integration and was used in synthetic feedback loops. Synthetic effector gene cassettes were integrated at the *LEU2* locus. Yeast promoters, terminator, and the PTP2 gene were PCR amplified from *Saccharomyces cerevisiae* genomic DNA (Invitrogen). YopH gene was a kind gift from Kim Orth. The OspF gene was synthesized by Integrated DNA Technologies, Inc. All yeast genomic integrations were confirmed by yeast colony PCR.

Flow cytometry experiments

Analysis of the pathway-dependent fluorescent proteins (GFP and mCherry) expression in yeast cells was preformed with the BD LSRII flow cytometer (BD Biosciences) equipped with a high-throughput sampler. For each experiment, triplicate cultures were grown in synthetic complete media to early log phase (OD_{600} = 0.1 – 0.2). At time = 0, 1.5 μM of α-factor (GenScript) or 0.4 M of KCl were added into parallel cultures to induce separately the mating- specific or osmo-specific pathway response. For mating response, 100 μL aliquots were taken at time = 0 and after 2 hours of induction; for osmotic response, 100 μL aliquots were taken at time = 0 and after 1 hour of induction. Each 100 μL sample aliquot was immediately mixed with 100 μL of cycloheximide (10 μg/mL) in 96-well plates to stop the protein synthesis. After incubating the samples at room temperature for 30 minutes in the dark to allow for the maturation of fluorescent proteins, the levels of fluorescence protein were determined by flow cytometry. For each read, 10,000 cells were counted, and the mean fluorescent density was calculated by Flowjo software (BD Biosciences) as the pathway output value and the standard deviation from triplicate experiments was indicated as the error bar.

Microfluidics, fluorescent microscopy, and image processing

Mircofluidic yeast cell culture was performed in Y04C plate with ONIX flow control system (Cellasic Corp)[2]. Cultures were grown to mid-log phase (OD_{600} = 0.2 – 0.8) in synthetic complete media. Cells were diluted to OD_{600} = 0.01 in 600 μL of fresh media and sonicated at a minimum set of 11% for 1 sec using Fisher Scientific model 500 sonicator with a 2 mm tip. Cells were loaded into the flow chamber pre-coated with

concanavalin A and flowed over by synthetic complete media for more than 20 min before applying the square pulse sequence. Pulse stimulation with salt media was performed by ONIX FG flow control software (Cellasic Corp) with the flow pressure of 8 psi. Image acquisition was performed with a TE2000-E automated inverted microscope (Nikon) with Perfect Focus and 100x oil immersion lens.

Background subtraction was performed first on all fluorescence images using ImageJ (http://imagej.nih.gov). The subsequent image analysis for both nuclear Hog1-GFP import and *pSTL1*-mCherry expression was performed with custom Matlab (Mathworks) software (developed by Kai-Yeung Lau from Chao Tang's lab at UCSF). For Hog1-GFP import analysis, cell boundaries were first determined from the bright field DIC images. Cell nuclei were segmented by mCherry labeled nuclear images. The nuclear and total cell GFP densities were calculated from the GFP fluorescent images. For *pSTL1*-mCherry expression, cell boundaries were determined the same way Hog1-GFP localization and mCherry densities were determined from the mCherry fluorescent images. For all frequency responses, 210 min long time course of pulse stimulation was performed and the maximum value of each time course was taken as the output of the stimulation frequency. The population average of over 50 - 100 cells was determined for each single measurement, and each experiment was repeated at least three times (see also **Supplementary Fig. 3c and 3d**) and the standard deviation was calculated with the three experimental repeats.

Jurkat T cell experiments

Cell line and plasmids

Jurkat T cell with *pNFAT*-EGFP (Neomysin resistant) stably integrated into the chromosome is a Weiss lab stock strain. All plasmids were made by using standard cloning techniques, AarI combinatorial cloning technique[1] and Gateway cloning technique (Invitrogen). See **Supplementary Tables** below for more cloning detail.

Culture condition

Jurkat was maintained in RPMI 1640 supplemented with 10% heat inactivated (HI) FBS (Invitrogen), extra L-glutamine (2 mM), penicillin, streptomycin, and G418 (2mg/mL, Invitrogen).

Transfection

Before transfection, *Jurkat* T cells were cultured in RPMI 1640 supplemented with 10% Heat inactivated fetal bovine serum (FBS) and glutamine (10G RPMI) for at least 1 day. For each transfection, 20 million cells were spun down, washed once with 10G RPMI, and resuspended in 300ul of 10G RPMI. 15μg of each plasmid was added to each transfection, vortexed briefly, and incubated at room temperature for 15 minutes. The cell/DNA mixture was then subject to electroporation (BioRad, square pulse, 300V, 10ms pulse, 0.4 cm cuvette). The cells were rested at room temperature for 10 minutes before resuspending in 10mL of 10G RPMI. The cells were allowed to recover overnight before performing further experiment. For transfection with plasmids that contain the *pTRE* promoter, the serum was switched to Tet-free serum.

T cell activation and doxycycline induction

T cell receptor was activated with a *Jurkat* specific anti-TCR antibody, C305 (ascites, UCSF antibody core) at 1:2000 dilution unless stated other wise at the cell density of 2.5million cell/mL (for most experiment) or 0.5 million cells/mL (for Dox inducible expression (100nM) of effectors experiment). Phorbol 12-myristate 13-acetate (25ng/mL) and ionomycin (1μM) was also used to activate T cell in some experiment. For the dose response curve, the highest dose of C305 is 1:600 and serially diluted 3 fold to generate 8 doses total.

Antibody staining and flow cytometry analysis

For staining of cell surface expression of CD69, cells were fixed, and stained with anti-CD69-APC (BD). For staining of phosphorylated ERK, cells were fixed, made permeable by incubation with ice-cold 90% methanol on ice for 30 minutes and stained with primary antibody to phosphorylated ERK (197G2; Cell Signaling) and anti-rabbit APC secondary antibody (711-136-152, Jackson Immunoresearch). All samples were analyzed with BD LSRII equipped with high throughput sampler. Live cells were determined from forward and side scattering. Transfected cells were determined by comparing cells without mCherry to cells transfected with *pEF*-mCherry. Only transfected and live cells were included in the analysis. Error bar represents the standard deviation from three samples.

Western blot to determine protein expression level

1 million live cells were quickly spun down and lysed on ice for 30min. The supernatant were then spun down at 4℃ for 30 min. The lysates were then mixed with DTT and SDS sample loading buffer and boiled for 3 minutes. Samples were separated with SDS PAGE gel (4-12% Bis-Tris) and then transferred to nitrocellulose blot. The blot were stained with primary anti-HA antibody (Santa Cruz Biotechnology) and Li-Cor anti-mouse 680 LT secondary antibody. The blot was imaged with the Li-Cor Odyssey.

Human primary CD4+ T cell experiments

Human primary CD4+ T cell transduction

Human peripheral blood mononuclear cells were collected from normal donors and acquired as cell suspensions from flushed TRIMA leukoreduction chambers (Blood Centers of the Pacific, San Francisco, CA). Primary CD4+ T cells were purified by negative selection and Ficoll-Paque PLUS density medium separation (RosetteSep, Stem Cell Technologies). Purified cells were cryopreserved and placed in liquid nitrogen storage.

Replication-incompetent lentiviral particles were prepared in 293T cells by standard methods. Briefly, constructs of interest were cloned into the transfer vector pHR'SIN:CSW using standard molecular biology techniques and then co-transfected into 293T cells along with the viral packaging plasmids pCMVdR8.91 and pMD2.G using the transfection reagent FuGENE HD (Roche). Amphotropic VSV-G pseudotyped lentiviral particles in the supernatant were collected 48 hours later.

Prior to use, human primary CD4+ T cells were thawed and cultured overnight in growth medium (X-VIVO 15 + 5% human AB serum + 10mM N-acetylcysteine + 1X beta-mercaptoethanol + 1X Primocin) supplemented with 30U/mL IL-2. The next day, cells were activated with Dynabeads human T-Activator CD3/CD28 (Invitrogen) at a 3:1

beads-to-cells ratio. After 24 hours of activation, the cells were transduced with lentiviral particles. In some cases, transduction was performed on RetroNectin-coated tissue culture plates to enhance viability and transduction efficiency. Briefly, non-tissue culture treated plates were coated with RetroNectin (32μg/mL) and then blocked with PBS + 2% BSA. Viral supernatant was loaded into the wells and the plate was centrifuged at 1200g for 1.5 hours at room temperature. Finally, wells were washed once with PBS, activated T cells were loaded into the wells, and the plate was once again centrifuged at 1200g for 1 hour with reduced braking speed. T cells were then placed into the 37℃ incubator.

Human primary CD4+ T cell IL-2 release assay

Transduced cells were rested by culturing them for greater than 10 days in the presence of 30U/mL IL-2 added every other day for maintenance. Doxycycline (200 ng/ml) was added to the cells and the cells were incubated for 6 hours. Cells were washed and 5e4 human primary CD4+ cells (transduced with the pause switch constructs or untransduced) were placed in a 96-well plate with 200 μL human growth media with activation agents added (10 ng/ml PMA + 0.5 μM ionomycin, magnetic Dynabeads coated with anti-CD3/anti-CD28 (beads/cells ratio, 0.3:1), or Raji B cells loaded with a superantigen cocktail). Doxycycline (200ng/mL) was added into appropriate wells. After 24 hours of incubation at 37℃, the released IL-2 in the supernatant was measured with the human IL-2 ELISA kit II (BD Biosciences).

Human primary CD4+ T cell proliferation assay

Resting primary CD4+ T cells were pretreated with 200 ng/ml doxycycline for 6 hours and then labeled with CellTrace Violet dye (Invitrogen). 5e4 dye-labeled human CD4+ T cells were placed in a 96-well plate with 200 μL human growth media in the presence or absence of doxycycline (200ng/mL) and Dynabeads coated with anti-CD3/anti-CD28 (beads/cells ratio, 0.3:1) to induce proliferation. After incubation at 37℃ for 4 days, the cells were assayed by flow cytometry. FlowJo curve fitting software was used to quantitate cell proliferation as indicated by dilution of the CellTrace Violet dye in proliferating cells.

Supplementary Computation Model

The simulation results shown in Supplementary Figure 2 and 3 are based on the computation model developed by Zi et al[3]. The following are the equations used for the wild type model (same as Zi et al). All the kinetic parameters are also the same as the model by Zi et al. The simulation were solved in MATLAB.

$$\frac{d[Pbs2]}{dt} = -\frac{K_{pho}^{Pbs2}\cdot[Pbs2]}{1+\left(\frac{PI_t}{\alpha}\right)^8} + K_{depho}^{Pbs2}\cdot[Pbs2PP] - [Pbs2]\cdot V_{ratio} \tag{1}$$

$$\frac{d[Pbs2PP]}{dt} = \frac{K_{pho}^{Pbs2}\cdot[Pbs2]}{1+\left(\frac{PI_t}{\alpha}\right)^8} - K_{depho}^{Pbs2}\cdot[Pbs2PP] - [Pbs2PP]\cdot V_{ratio} \tag{2}$$

$$\begin{aligned}\frac{d[Hog1c]}{dt} = &-K_{pho}^{Hog1}\cdot[Pbs2PP]\cdot[Hog1c] + K_{depho}^{Hog1PPc}\cdot[Hog1PPc] \\ &- K_{imp}^{Hog1c}\cdot[Hog1c] + \frac{K_{exp}^{Hog1n}\cdot[Hog1n]\cdot V_{nuc}}{V_{cyt}} - [Hog1c]\cdot V_{ratio}\end{aligned} \tag{3}$$

$$\begin{aligned}\frac{d[Hog1PPc]}{dt} = &K_{pho}^{Hog1}\cdot[Pbs2PP]\cdot[Hog1c] - K_{depho}^{Hog1PPc}\cdot[Hog1PPc] \\ &- K_{imp}^{Hog1PPc}\cdot[Hog1PPc] + \frac{K_{exp}^{Hog1PPn}\cdot[Hog1PPn]\cdot V_{nuc}}{V_{cyt}} \\ &- [Hog1PPc]\cdot V_{ratio}\end{aligned} \tag{4}$$

$$\begin{aligned}\frac{d[Hog1n]}{dt} = &\frac{K_{imp}^{Hog1c}\cdot[Hog1c]\cdot V_{cyt}}{V_{nuc}} - K_{exp}^{Hog1n}\cdot[Hog1n] + K_{depho}^{Hog1PPn}\cdot[Hog1PPn] \\ &- [Hog1n]\cdot V_{ratio}\end{aligned} \tag{5}$$

$$\frac{d[Hog1PPn]}{dt} = \frac{K_{imp}^{Hog1PPc} \cdot [Hog1PPc] \cdot V_{cyt}}{V_{nuc}} - K_{exp}^{Hog1PPn} \cdot [Hog1PPn] - K_{depho}^{Hog1PPn} \cdot [Hog1PPn] - [Hog1PPn] \cdot V_{ratio} \quad (6)$$

$$\frac{d[Glyc\_in]}{dt} = K_{s0}^{Glyc} + \frac{K_{s1}^{Glyc} \cdot (totalHog1PP)^4}{\beta^4 + (totalHog1PP)^4} + K_{s2}^{Glyc} \cdot [Yt] - \left(K_{exp0}^{Glyc} + \frac{K_{exp1}^{Glyc} \cdot (PI_t)^{12}}{(\gamma)^{12} + (PI_t)^{12}} \right) \cdot ([Glyc\_in] - [Glyc\_ex]) - [Glyc\_in] \cdot V_{ratio} \quad (7)$$

$$\frac{d[Yt]}{dt} = K_{s0}^{Yt} + K_{s1}^{Yt} \cdot [z4] - K_t^{Yt} \cdot [Yt] - [Yt] \cdot V_{ratio} \quad (8)$$

$$\frac{d[z1]}{dt} = \frac{4 \cdot ([Hog1PPn] - [z1])}{\tau} \quad (9)$$

$$\frac{d[z2]}{dt} = \frac{4 \cdot ([z1] - [z2])}{\tau} \quad (10)$$

$$\frac{d[z3]}{dt} = \frac{4 \cdot ([z2] - [z3])}{\tau} \quad (11)$$

$$\frac{d[z4]}{dt} = \frac{4 \cdot ([z3] - [z4])}{\tau} \quad (12)$$

$$\frac{d(V_{os})}{dt} = -G \cdot Lp \cdot (PI_e + PI_t - PI_i) \quad (13)$$

$$PI_e = PI_e^0 + w \cdot [NaCl] \quad (14)$$

$$PI_t = \begin{cases} \dfrac{PI_t^0 \cdot (V_{os} - V_{os}^{PI_t=0})}{(V_{os}^0 - V_{os}^{PI_t=0})} & \text{if } V_{os}^0 > V_{os}^{PI_t=0} \\ 0 & \text{if } V_{os}^0 \le V_{os}^{PI_t=0} \end{cases} \quad (15)$$

$$V_{cell} = V_{os} + V_b \quad (16)$$

$$V_{cyt} = f^{V_{cyt}} \cdot V_{cell} = 0.5 \cdot V_{cell} \tag{17}$$

$$V_{nuc} = f^{V_{nuc}} \cdot V_{cell} = 0.07 \cdot V_{cell} \tag{18}$$

$$PI_i = \frac{n \cdot R \cdot T}{V_{os}} = \frac{n_0 + n_{Glyc}}{V_{os}} \cdot R \cdot T = \frac{n_0 + [Glyc\_in] \cdot V_{cyt}}{V_{os}} \cdot R \cdot T$$
$$= \frac{n_0 + [Glyc\_in] \cdot V_{cyt}}{V_{os}} \cdot 10^{-9} \cdot 8.314 \cdot 303.15 \tag{19}$$

$$totalHog1PP = \frac{([Hog1PPc] \cdot V_{cyt} + [Hog1PPn] \cdot V_{nuc}) \cdot 602}{6780} \tag{20}$$

$$V_{ratio} = \frac{1}{V_{cell}} \cdot \frac{d(V_{cell})}{dt} = \frac{1}{V_{cell}} \cdot \frac{d(V_{os} + V_b)}{dt} = \frac{1}{V_{cell}} \cdot \frac{d(\cdot V_{os})}{dt}$$
$$= \frac{-G \cdot Lp \cdot (PI_e + PI_t - PI_i)}{V_{cell}} \tag{21}$$

$$Rt = \frac{[Hog1n] + [Hog1PPn]}{\frac{\left(\frac{N_{Hog1}^{total}}{N_a}\right)}{(V_{cell} - V_{cell}^{wall})}}$$
$$= \frac{([Hog1n] + [Hog1PPn]) \cdot 0.8 \cdot (Vos + Vb) \cdot 602}{6780} \tag{22}$$

(note: $[Hog1n]$ and $[Hog1PPn]$ have unit of 10^{-6} M; V_{cell} has unit of 10^{-15} L)

For the computation model that contains the reversible feedback loop, equations involving the cytoplasmic Hog1 were changed to account for the modification of Hog1 by the effector. Only cytomplasmic Hog1 is affected directly by the effector. Another equation was added to account for the expression of the effector by nuclear phosphorylated Hog1.

$$\frac{d[Hog1c]}{dt} = -K_{pho}^{Hog1} \cdot [Pbs2PP] \cdot [Hog1c] + K_{depho}^{Hog1PPc} \cdot [Hog1PPc] - K_{imp}^{Hog1c} \cdot [Hog1c] + \frac{K_{exp}^{Hog1n} \cdot [Hog1n] \cdot V_{nuc}}{V_{cyt}} - [Hog1c] \cdot V_{ratio} + \alpha_1 \cdot [Hog1PPc] \cdot [Effector] \quad (23)$$

$$\frac{d[Hog1PPc]}{dt} = K_{pho}^{Hog1} \cdot [Pbs2PP] \cdot [Hog1c] - K_{depho}^{Hog1PPc} \cdot [Hog1PPc] - K_{imp}^{Hog1PPc} \cdot [Hog1PPc] + \frac{K_{exp}^{Hog1PPn} \cdot [Hog1PPn] \cdot V_{nuc}}{V_{cyt}} - [Hog1PPc] \cdot V_{ratio} - \alpha_1 \cdot [Hog1PPc] \cdot [Effector] \quad (24)$$

$$\frac{d[Effector]}{dt} = \frac{\alpha_{14} [Hog1PPn]^n}{K_{14}{}^n + [Hog1PPn]^n} - [Effector] \cdot V_{ratio} \quad (25)$$

For the model that contains the irreversible feedback loop, the equations involving the cytoplasmic phosphorylated Hog1 were changed, but not the non-phosphorylated Hog1. Instead, a new specice of dead Hog1 (Hog1Dead) appears and a new equation was added to describe the dynamics of this specie of Hog1. Furthermore, even though Hog1Dead cannot participate in transcription response and be phosphorylatd again, it is still fluorescence and may be translocated into nucleus similar to non-phosphorylated Hog1. Threfore the equation that describe the level of total nuclear Hog1 was modified to include new Hog1Dead.

$$\frac{d[Hog1PPc]}{dt} = K_{pho}^{Hog1} \cdot [Pbs2PP] \cdot [Hog1c] - K_{depho}^{Hog1PPc} \cdot [Hog1PPc] - K_{imp}^{Hog1PPc} \cdot [Hog1PPc] + \frac{K_{exp}^{Hog1PPn} \cdot [Hog1PPn] \cdot V_{nuc}}{V_{cyt}} - [Hog1PPc] \cdot V_{ratio} - \alpha_1 \cdot [Hog1PPc] \cdot [Effector] \quad (26)$$

$$\frac{d[Hog1Deadc]}{dt} = -K_{imp}^{Hog1c} \cdot [Hog1Deadc] + \frac{K_{exp}^{Hog1n} \cdot [Hog1Deadn] \cdot V_{nuc}}{V_{cyt}} - [Hog1Deadc] \cdot V_{ratio} + \alpha_1 \cdot [Hog1PPc] \cdot [Effector] \quad (27)$$

$$\frac{d[Hog1Deadn]}{dt} = +K_{imp}^{Hog1c} \cdot [Hog1Deadc] - \frac{K_{exp}^{Hog1n} \cdot [Hog1Deadn] \cdot V_{nuc}}{V_{cyt}} - [Hog1Deadn] \cdot V_{ratio} \quad (28)$$

$$\frac{d[Effector]}{dt} = \frac{\alpha_{14} [Hog1PPn]^n}{K_{14}{}^n + [Hog1PPn]^n} - [Effector] \cdot V_{ratio} \quad (29)$$

$$Rt = \frac{[Hog1n] + [Hog1PPn] + [Hog1Deadn]}{\frac{\left(\frac{N_{Hog1}^{total}}{N_a}\right)}{(V_{cell} - V_{cell}^{wall})}} = \frac{([Hog1n] + [Hog1PPn] + [Hog1Deadn]) \cdot 0.8 \cdot (Vos + Vb) \cdot 602}{6780} \quad (30)$$

The goal of this model is to compare the outcome of reversible modification to irreversible modification, therefore the parameters for the enzyme kinetics and gene express dynamics are the same for both the reversible and irreversible effectors. The parameters were chosen to qualitatively match experimental results.

For figure S2, the parameters are

$\alpha_1 = 0.1$, $\alpha_{14} = 0.3$, $K_{14} = 0.08$, n=10, μ=0.01.

For **Supplementary Figure 2**, the heat map parameters ranges are

Effector (maximum) enzyme activity: α_1 = 0.01-10,

Effector (maximum) gene expression rate: α_{14} = 0.05 – 10,

Effector degradation rate μ =0.0005 - 0.5

Supplementary Table 1 Plasmids used in yeast experiments

Plasmid	Parent vector	Promoter	Epitope	Gene	Leucine zipper[4]
WP201	pNH605	*pCYC1*	3xFlag	OspF	adapter
WP202	pNH605	*pCYC1*	3xFlag	OspF (K134A)	adapter
WP203	pNH605	*pCYC1*	3xFlag	ΔN-OspF	adapter
WP204	pNH605	*pCYC1*	3xFlag	ΔN-OspF	EE
WP205	pNH605	*pCYC1*	3xFlag	ΔN-OspF	RR
WP206	pNH605	*pCYC1*	3xFlag	ΔN-OspF(K134A)	EE
WP207	pNH605	*pSTL1*	3xFlag	ΔN-OspF	EE
WP208	pNH605	*pSTL1*	3xFlag	PTP2	EE

Supplementary Table 2 Yeast strains used in this study

Strain	*Description*
SP147	*W303 MATa, bar1::NatR, far1Δ, mfa2::pFUS1-GFP, HO::pSTL1-mCherry, his3, trp1, leu2, ura3*
WP020	*W303 MATa, bar1::NatR, far1Δ, mfa2::pFUS1-GFP, HO::pSTL1-mCherry, pbs2::URA3, his3, trp1, leu2, ura3*
WP022	*W303 MATa, bar1::NatR, far1Δ, mfa2::pFUS1-GFP, HO::pSTL1-mCherry, Pbs2::Pbs2-zipper(RR), his3, trp1, leu2, ura3*
WP116	*W303 MATa, bar1::NatR, far1Δ, mfa2::pFUS1-GFP, HO::pSTL1-mCherry, Ste5::Ste5-zipper(EE), his3, trp1, leu2, ura3*
WP038	*W303 MATa, Trp1::pADH1-Htb2-mCherry, Hog1::Hog1-GFP, pbs2::URA3, his3, trp1, leu2, ura3*
WP039	*W303 MATa, Trp1::pADH1-Htb2-mCherry, Hog1::Hog1-GFP, Pbs2::Pbs2-zipper(RR), his3, trp1, leu2, ura3*

Supplementary Table 3. Expression vectors used in the study with *Jurkat* T cell

Expression Vectors

Vector	Vector Name	Vector Source		Promoter	Gene	Cloning methods
1	pEF-HA-OspF	pEF/FRT/V5/DEST	Invitrogen	EF1-alpha	HA-OspF	Invitrogen's gateway recombination (LR clonase II) with pEF/FRT/V5/DEST and pENTR HA-OspF
2	pEF-HA-YopH	pEF/FRT/V5/DEST	Invitrogen	EF1-alpha	HA-YopH	Invitrogen's gateway recombination (LR clonase II) with pEF/FRT/V5/DEST and pENTR HA-YopH
3	pEF-HA-SHP-1	pEF/FRT/V5/DEST	Invitrogen	EF1-alpha	HA-SHP-1	Invitrogen's gateway recombination (LR clonase II) with pEF/FRT/V5/DEST and pENTR HA-SHP1
4	pNFAT-HA-OspF	p4XNFAT DEST	Arthur Weiss	4XNFAT	HA-OspF	Invitrogen's gateway recombination (LR clonase II) with pNFAT-DEST and pENTR HA-OspF
5	pNFAT-HA-YopH	p4XNFAT DEST	Arthur Weiss	4XNFAT	HA-YopH	Invitrogen's gateway recombination (LR clonase II) with pNFAT-DEST and pENTR HA-YopH
6	pAP1-HA-OspF	pAP1-DEST	Clontech	3XAP-1	HA-OspF	Invitrogen's gateway recombination (LR clonase II) with pAP1-DEST and pENTR HA-OspF
7	pAP1-HA-YopH	pAP1-DEST	Clontech	3XAP-1	HA-YopH	Invitrogen's gateway recombination (LR clonase II) with pAP1-DEST and pENTR HA-YopH
8	pNFAT-HA-OspF-PEST	p4XNFAT DEST	Arthur Weiss	4XNFAT	HA-OspF-PEST	Invitrogen's gateway recombination (LR clonase II) with pNFAT-DEST and pENTR HA-OspF-PEST
9	pNFAT-HA-YopH-PEST	p4XNFAT DEST	Arthur Weiss	4XNFAT	HA-YopH-PEST	Invitrogen's gateway recombination (LR clonase II) with pNFAT-DEST and pENTR HA-YopH-PEST
10	pAP1-HA-OspF-PEST	pAP1-DEST	Clontech	3XAP-1	HA-OspF-PEST	Invitrogen's gateway recombination (LR clonase II) with pAP1-DEST and pENTR HA-OspF-PEST
11	pAP1-HA-YopH-PEST	pAP1-DEST	Clontech	3XAP-1	HA-YopH-PEST	Invitrogen's gateway recombination (LR clonase II) with pAP1-DEST and pENTR HA-YopH-PEST
12	pTRE-DD-OspF	pTRE-DEST	Clontech	TRE	DD-OspF	Invitrogen's gateway recombination (LR clonase II) with pTRE-DEST and pENTR DD-OspF
13	pTRE-DD-YopH	pTRE-DEST	Clontech	TRE	DD-YopH	Invitrogen's gateway recombination (LR clonase II) with pAP1-DEST and pENTR DD-YopH
14	pEF-mCherry	pEF/FRT/V5/DEST	Invitrogen	EF1-alpha	mCherry	Invitrogen's gateway recombination (LR clonase II) with pEF/FRT/V5/DEST and pENTR-mCherry
15	pEF-HA-GST	pEF/FRT/V5/DEST	Invitrogen	EF1-alpha	GST-HA	Invitrogen's gateway recombination (LR clonase II) with pEF/FRT/V5/DEST and pENTR-GST-HA
16	pEF/pTetON	pEF/FRT/V5/DEST	Invitrogen	CMV	Tet-ON Advanced (rtTA)	The expression cassett of pCMV-Tet-ON Advanced was PCR amplified from pTet-ON Advanced. The amplified fragement was then cloned into pEF/FRT/V5 DEST between the restriction site Acc65I and SphI
17	pEF-HA-OspF K134A	pEF/FRT/V5/DEST	Invitrogen	EF1-alpha	HA-OspFK134A	Invitrogen's gateway recombination (LR clonase II) with pEF/FRT/V5/DEST and pENTR HA-OspFK134A
18	pEF-HA-YopH C403A	pEF/FRT/V5/DEST	Invitrogen	EF1-alpha	HA-YopHC403A	Invitrogen's gateway recombination (LR clonase II) with pEF/FRT/V5/DEST and pENTR HA-YopHC403A

The DD in plasmid 12 and 13 is a destabilization domain based described by Banaszynski et al[5]. This domain was chosen because of it low basal expression level.

Supplementary Table 4. Gateway donor vector used to generate the expression vector

Donor Vectors Vector Name	Vector Source		Promoter	Gene	Cloning methods
pENTR-HA-OspF	pENTR (pDONR221)	Invitrogen	-	HA-OspF	All fusion proteins were constructed using the AarI cloning method described in Peisajovich et al. Briefly, the pDONR221 is modified to include the AarI cloning sites between the attB1 and attB2 recomination sites. After digestion with AarI, fragments are ligated using standard cloning technique.
pENTR-HA-YopH	pENTR (pDONR221)	Invitrogen	-	HA-YopH	
pENTR-HA-SHP-1	pENTR (pDONR221)	Invitrogen	-	HA-SHP-1	
pENTR-HA-OspFK134A	pENTR (pDONR221)	Invitrogen	-	HA-OspFK134A	
pENTR-HA-YopHC403A	pENTR (pDONR221)	Invitrogen	-	HA-YopHC403A	
pENTR-HA-OspF-PEST	pENTR (pDONR221)	Invitrogen	-	HA-OspF-PEST	
pENTR-HA-YopH-PEST	pENTR (pDONR221)	Invitrogen	-	HA-YopH-PEST	
pENTR-DD-OspF	pENTR (pDONR221)	Invitrogen	-	DD-OspF	
pENTR-DD-YopH	pENTR (pDONR221)	Invitrogen	-	DD-YopH	
pENTR-GST-HA	pENTR (pDONR221)	Invitrogen	-	GST-HA	
pENTR-mCherry	pENTR (pDONR221)	Invitrogen	-	mCherry	This construct was made using the gateway cloning strategy

Supplementary Table 5. Gateway destination vector used to generate the expression vector

Destination Vectors Vector Name	Vector Source
pNFAT(d2)-DEST	pNFAT-GFP
pAP1-DEST	pAP1-Luc
pEF/FRT/V5/DEST	pEF/FRT/V5/DEST
pTRE-DEST	pTRE-Tight

Supplementary Table 6. Other vectors used to generate the expression vector

Other Vectors Vector Name	Vector Source		Promoter	Gene	Cloning methods
pTuner-OspF	pTuner	Clontech	CMV	OspF	Using standard cloning technique, OspF was cloned between the XhoI and BamHI site
pTuner-YopH	pTuner	Clontech	CMV	YopH	Using standard cloning technique, OspF was cloned between the XhoI and BamHI site
pTet-ON Advanced	pTet-ON Advanced	Clontech	CMV	Tet-ON Advanced	No modification made

Supplementary Table 7. Plasmids used in the transfection*

Figure #	Sample	Plasmid A	Plasmid B
Figure 3A	pEF-HA-YopH	2	-
	pEF-HA-OspF	1	-
	WT	15	-
Figure 3B	pNFAT-HA-OspF	4	-
	pNFAT-HA-OspF-PEST	8	-
	pEF-HA-OspF	1	-
	WT	15	-
Figure 3C, S8	pTRE-DD-Yop	13	16
	pTRE-DD-OspF	12	16
	WT	15	16
Figure S5A, S5C	pEF-YopH	2	-
	pEF-OspF	1	-
	pEF-SHP-1	3	-
	WT	14	-
Figure S7	pNFAT-HA-OspF	4	-
	pNFAT-HA-OspF-PEST	8	-
	pAP1-HA-OspF	6	-
	pAP1-HA-OspF-PEST	10	-
	pNFAT-HA-YopH	5	-
	pNFAT-HA-YopH-PEST	9	-
	pAP1-HA-YopH	7	-
	pAP1-HA-YopH-PEST	11	-
	pEF-HA-YopH	2	-
	pEF-HA-OspF	1	-
	WT	15	-
Figure S5B	pEF-YopH	1	-
	pEF-YopHC403A	18	-
	pEF-OspF	2	-
	pEF-OspFK134A	17	-
	WT	15	-

- A *pEF*-mCherry plasmid (13) is used in all transfection as transfection efficiency marker. The identity of plasmid number can be found in Supplementary Table 3.

Supplementary Table 8. Plasmids used in the human primary CD4+ T cell experiments

Plasmid	Parent vector	Gene
pHR-rtTA	pHR'SIN:CSW	Tet-ON Advanced
pHR-TRE-DD-OspF	pHR'SIN:CSW	Tet-inducible OspF

Supplemental References

1. Peisajovich, S. G., Garbarino, J. E., Wei, P. & Lim, W. A. Rapid diversification of cell signaling phenotypes by modular domain recombination. *Science* **328**, 368-72 (2010).
2. Lee, P. J., Helman, N. C., Lim, W. A. & Hung, P. J. A microfluidic system for dynamic yeast cell imaging. *BioTechniques* **44**, 91-5 (2008).
3. Zi, Z., Liebermeister, W. & Klipp, E. A quantitative study of the Hog1 MAPK response to fluctuating osmotic stress in Saccharomyces cerevisiae. *PloS one* **5**, e9522 (2010).
4. Bashor, C. J., Helman, N. C., Yan, S. & Lim, W. A. Using engineered scaffold interactions to reshape MAP kinase pathway signaling dynamics. *Science* **319**, 1539-43 (2008).
5. Banaszynski, L. A., Chen, L. C., Maynard-Smith, L. A., Ooi, A. G. & Wandless, T. J. A rapid, reversible, and tunable method to regulate protein function in living cells using synthetic small molecules. *Cell* **126**, 995-1004 (2006).

Pathogen effectors can be harnessed to inhibit specific MAPKs through scafold protein recruitment with leucine zippers in yeast

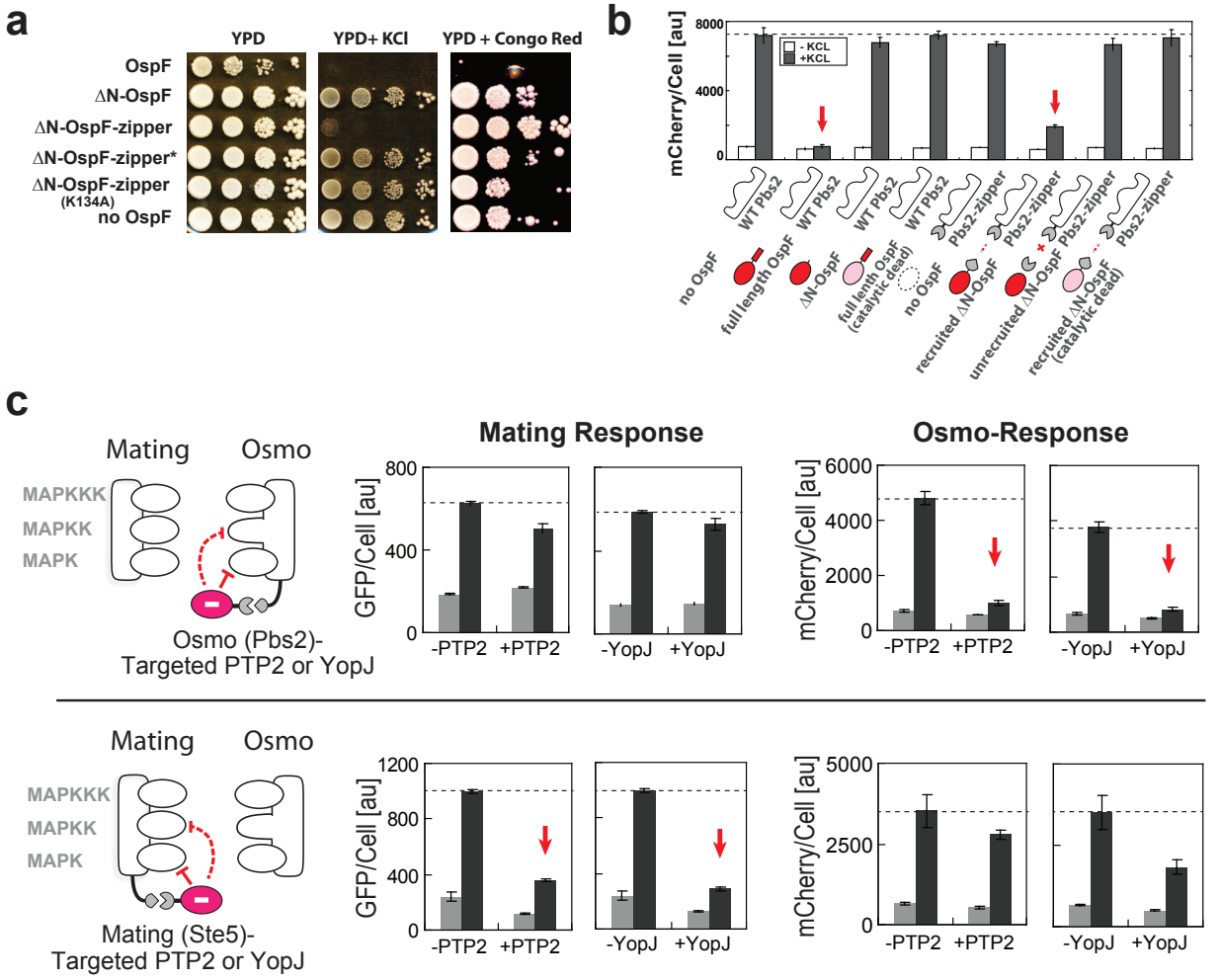

Supplementary Figure 1. Engineering effectors that specifically block the MAPK pathways. a, Yeast cells with variants of OspF were plated on YPD (left), YPD with 1 M KCl (middle), and YPD with 30 μg/ml congo red (right) plates. Variants include wild type OspF, ΔN-OspF, ΔN-OspF with zipper, ΔN-OspF with nonbinding zipper (zipper*), catalytic dead ΔN-OspF (K134A) with zipper and cells without OspF (No OspF). **b,** The transcriptional osmo-responses (as reported by *pSTL1*-mCherry) were measured at 1 hour after stimulated with 0.4 M KCl. All variant of OspFs were expressed by the *pCYC1* promoter and integrated into yeast genome; Pbs2 variants were integrated and expressed from endogenous Pbs2 locus. Only the OspF variants that are recruited to Hog1/Pbs2 display selective inhibition. Catalytic activity of OspF and functional zippers are required for inhibition using ΔN-OspF (no docking motif). **c,** PTP2, a yeast endogenous protein tyrosine phosphatase, and YopJ, a *Yersinia* MAPKK acetyltransferase, were engineered to selectively inhibit mating or osmo-MAPK pathway with leucine zipper based MAPK pathway recruitment. *pAHD1* promoter was used to constitutively express PTP2-zipper, while *pCYC1*-promoter was used to drive the constitutive expression of YopJ.

Simulations indicate that irreversible effector feedback loop will more robustly filter HOG MAPK pathway output upon intermediate frequency stimulation

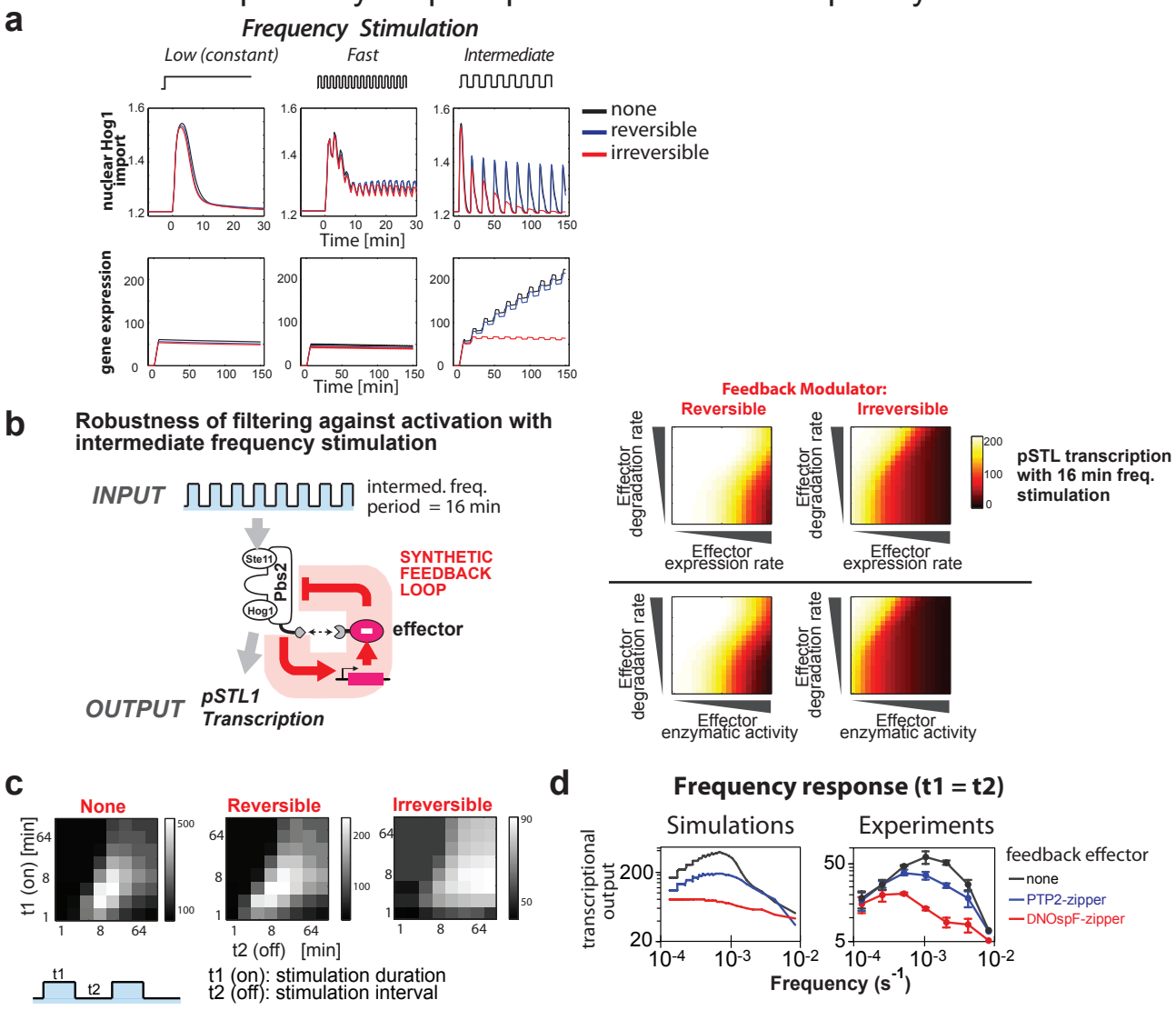

Supplementary Figure 2. Simulation indicates that synthetic negative feedback loops can alter the frequency dependent activation of the HOG MAPK pathway. **a,** Hog1 translocation into the nucleus and *pSTL1* transcription activity with feedback loops under periodic simulation. The simulation for control cells (black line) is based on the model by Zi et. al. and described in supplemental data. The model with a reversible feedback loop (blue line) uses the WT model with an additional transcription feedback loops expressing effectors that convert activated Hog1 into inactive form. The model with an irreversible feedback loop (red line) is the same as the reversible feedback loop, except the effectors modifies activated Hog1 into a dead Hog1 that cannot be phosphorylated again. See Supplementary Model for more details. Simulations are shown for constant stimulation, stimulation at high frequency (2 min period) and intermediate frequency (16 min period). **b,** The gene expression from an osmostress pathway transcriptional reporter upon stimulation with 16 minute period input was calculated. Plots show the dependence of reporter gene expression as a function of the properties of the negative feedback effector, i.e. effector expression rate, degradation rate, and enzymatic activity. Both reversible and irreversible enzyme can filter out this frequency input, but an irreversible effector can perform the task over much wider parameter range than a reversible effector. **c,** The model simulation suggested irrversible regulated cells introduced novel transcriptional reponse pattern with varying stimulation duration (on, t1) and interval time (off, t2). **d,** The model simulated the frequency dependent transcriptional response (t1 = t2) of the cells with no effector control (dark grey), with PTP2-zipper feedback (blue), and with OspF feedback (red). The transcriptional frequency response was also measured by experiments.

Characterization of the single cell fluorescence microscopy assay and the microfluidic control

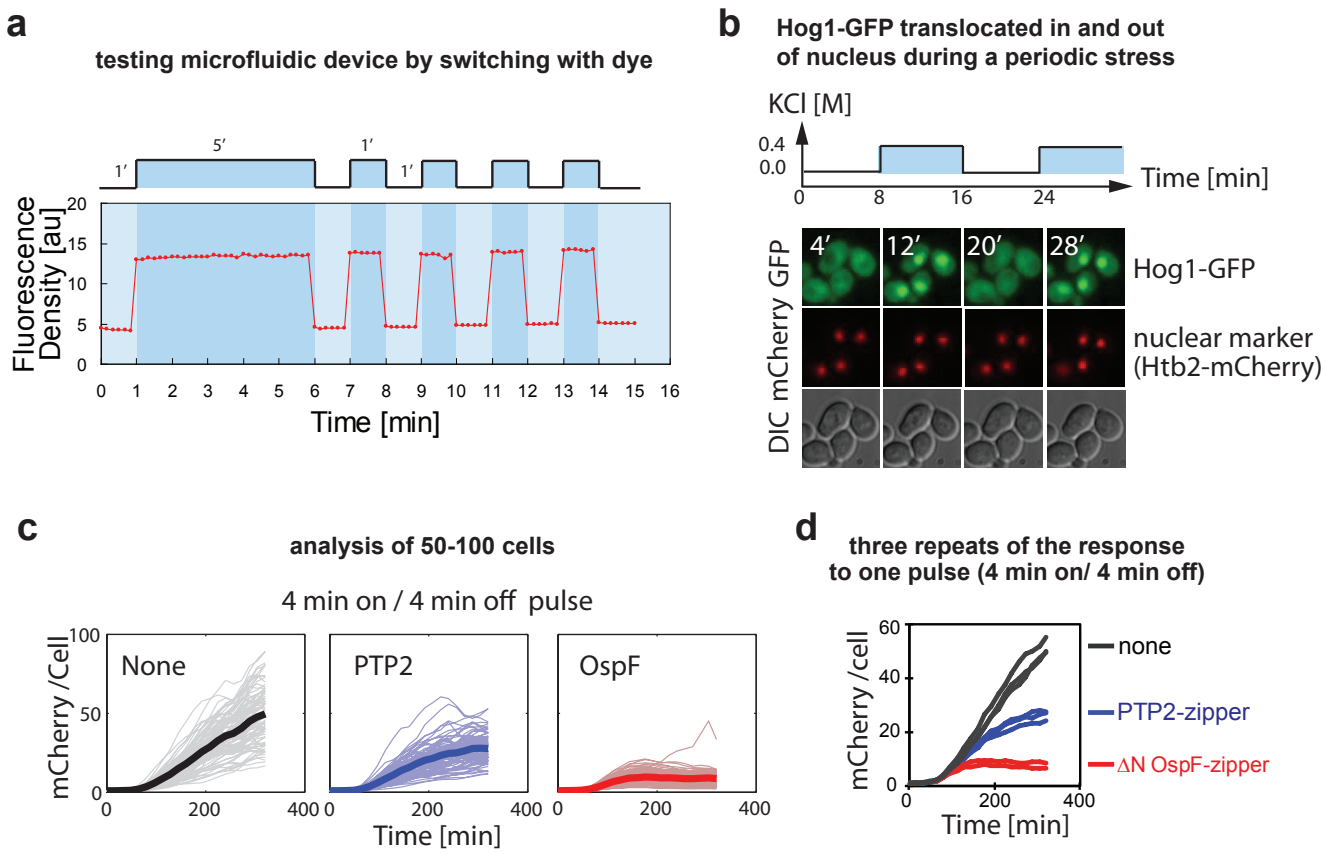

Supplementary Figure 3. Single cell assaying with microfluidic device. a, Cellasic microfluidic device can switch media effectively within 10 seconds. The fluorescent dye, Texas Red, was added into the SD-complete media with 0.4 M KCl (on) to visualize the flow-swithing. The SD-complete media with no KCl was as "off". A 5 min "on" followed by 4 cycles of 1 min "on" and 1 min "off" pulses was performed in a Cellasic Y04C plate with the flow-control pressure of 8 psi. The fluoresence density was calculated with ImageJ. **b,** Hog1 fused with GFP at the C-terminus is imported into nucleus when exposed to synthetic complete media with 0.4 M KCl and exported out of the nucleus following expose to media without KCl. Htb2 fused with mCherry at C-terminus constitutively expressed by *pADH1* was used to visualize the nucleus. Automated analysis of fractional import of Hog1 is described in Methods. **c,** For transcriptional activity assay, an average of 50 - 100 live cells was calculated. **d,** Each frequency data set was measured at least 3 times separately to calculate the standard deviation. An example frequency point, 4 min on/4 min off is shown.

Negative feedback regulation slightly accelerated the osmo-adaptation at both low and high stress, and feedback loop with OspF rendered the cell less responsive to a second step of osmostress.

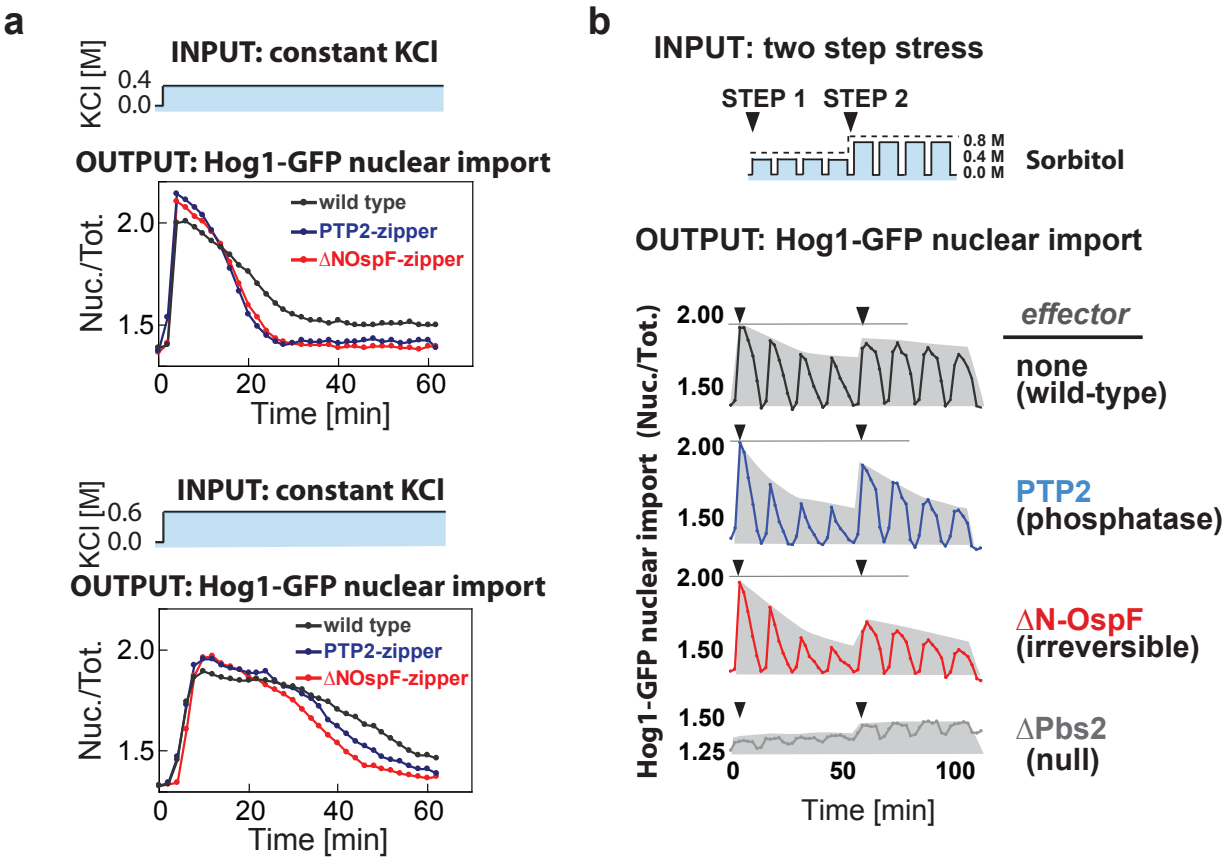

Supplementary Figure 4. OspF mediated feedback renders the cell less responsive to a second step of osmostress stimulation. a, Wild type (grey), PTP2 (blue) and ΔN-OspF(red) cells were stimulated with constant KCl (0.4M or 0.6M). The Hog1-GFP nuclear import was measued as the output of the activation of osmotic response. **b,** Cells were stimulated with 0.4 M sorbitol for 10 min with 4 min interval for four cycles, followed by a subsequent simulation with 0.8 M sorbitol for another four cycles. A time course of nuclear Hog1-GFP accumulation was recorded. We found that after four pulses of 0.4 M sorbitol, both the PTP2 and OspF negative feedback strains showed a dramatic decrease in Hog1 that could be imported to the nucleus (indicative of similar deactivation of phospho-Hog1 by both effectors). However, upon a second step up to higher osmolarity (0.8 M sorbitol), the PTP2 feedback strain was able to re-elicit a high level of Hog1 import, while the OspF feedback strain was not. These results are consistent with PTP2 converting phospho-Hog1 into dephosphorylated Hog1, which still remains competent for re-phosphorylation upon a further increase in MAPKK activity. In contrast, very little of the Hog1 population in the OspF strain was competent for rapid reactivation. These results are consistent with the OspF irreversibly depleting the pool of activatable Hog1 (except for new synthesis).

YopH and OspF inhibits T cell activation when induced with an anti-TCR antibody, while overexpression of mammalian SHP-1 phosphatase does not inhibit T cell response.

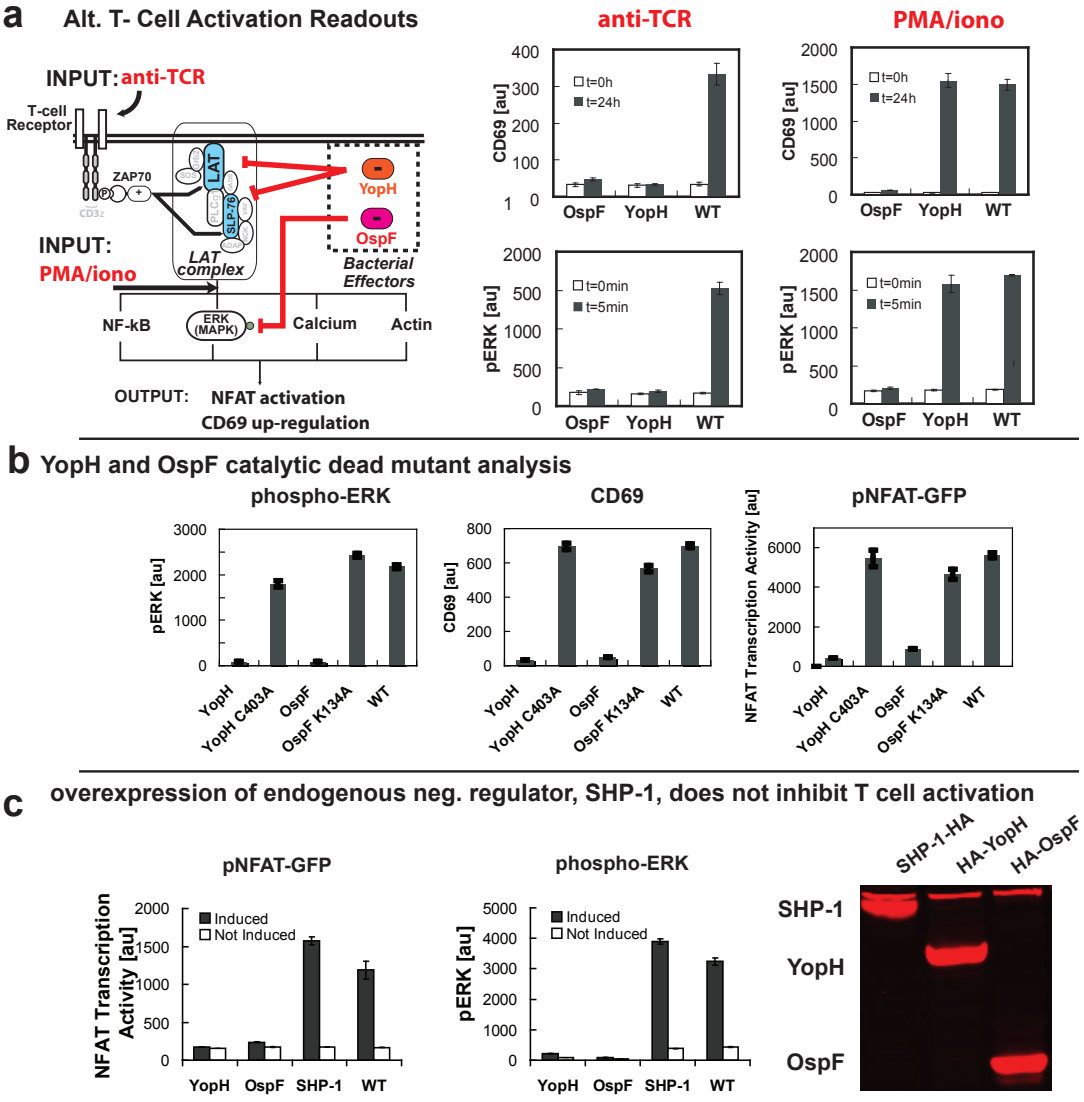

Supplementary Figure 5. Other TCR responses - ERK activation and CD69 expression - were also inhibited by YopH and OspF when cells are induced with an anti-TCR antibody (C305), while overexpression of mammalian SHP-1 phosphatase does not inhibit T cell response. a, Similar to the responses observed with NFAT transcription activation, YopH has no effect on phospho-ERK and CD69 upregulation when T cells were induced with PMA/ionomycin. **b,** Catalytic dead mutant of YopH (YopH C403A) and OspF (OspF K134A) have no effect on TCR activation (induced with C305) as measured by phospho-ERK, CD69 and NFAT transcription activation. **c,** Comparison of the effect of SHP-1 overexpression to YopH and OspF on TCR activation, as measured by NFAT transcription activity and phospho-ERK. (right) Expression level of proteins measured by Western blot against the HA epitope tag. Overexpression the mammalian phosphatase SHP-1, did not inhibit TCR activation most likely because SHP-1 is autoinhibited and subjected to complex regulation. This regulatory complexity is one of the challenges of using endogenous pathway modulators. In general, bacterial effectors may be easier to use as synthetic biology reagents for rewiring mammalian signaling.

Specific OspF mutant can be used to derive negative regulator that is specific for pERK vs pp38 MAPK inhibition in Jurkat T cells.

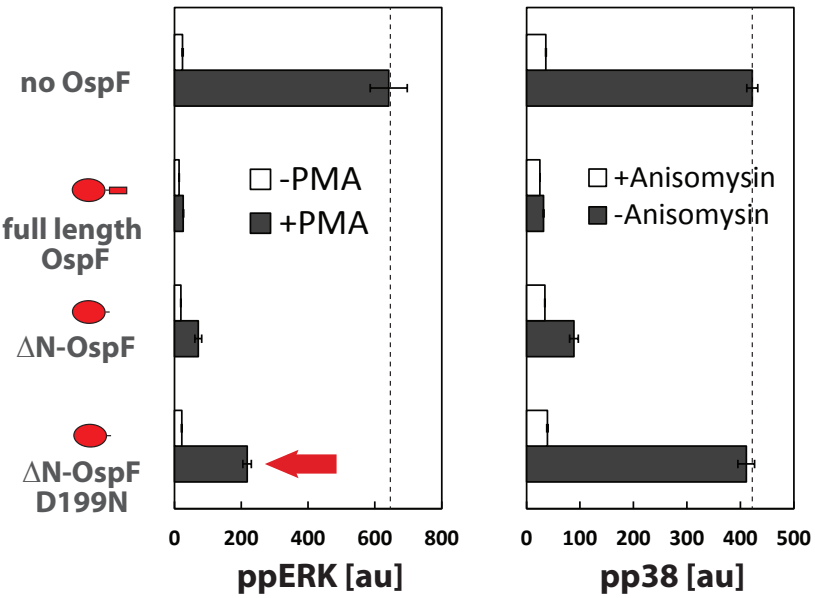

Supplementary Figure 6: Specific OspF mutant can be used to derive negative regulator that is specific for pERK vs pp38 MAPK inhibition in Jurkat T cells. Jurkat T cells were transfected with OspF and various mutants (all fused to mCherry at the N terminus). The ERK pathway was induced with PMA while the p38 pathway was induced with anisomysin. The level of pERK (left) and pp38 (right) was measured by phosphoflow with antibody against ppERK (Cell Signaling 4370) or pp38 (Cell Signaling 4511). Only cells with low OspF expression level (as determined by mCherry level) were included in the analysis. Full length wild type OspF and ΔN-OspF are very active toward both ERK and p38. The D199N mutant, however, is biased toward ERK when expressed at low level.

Mechanism of amplitude limiter circuit: Introduction of OspF negative feedback loop causes transient Erk activation (instead of sustained), leading to lower steady pathway output amplitude

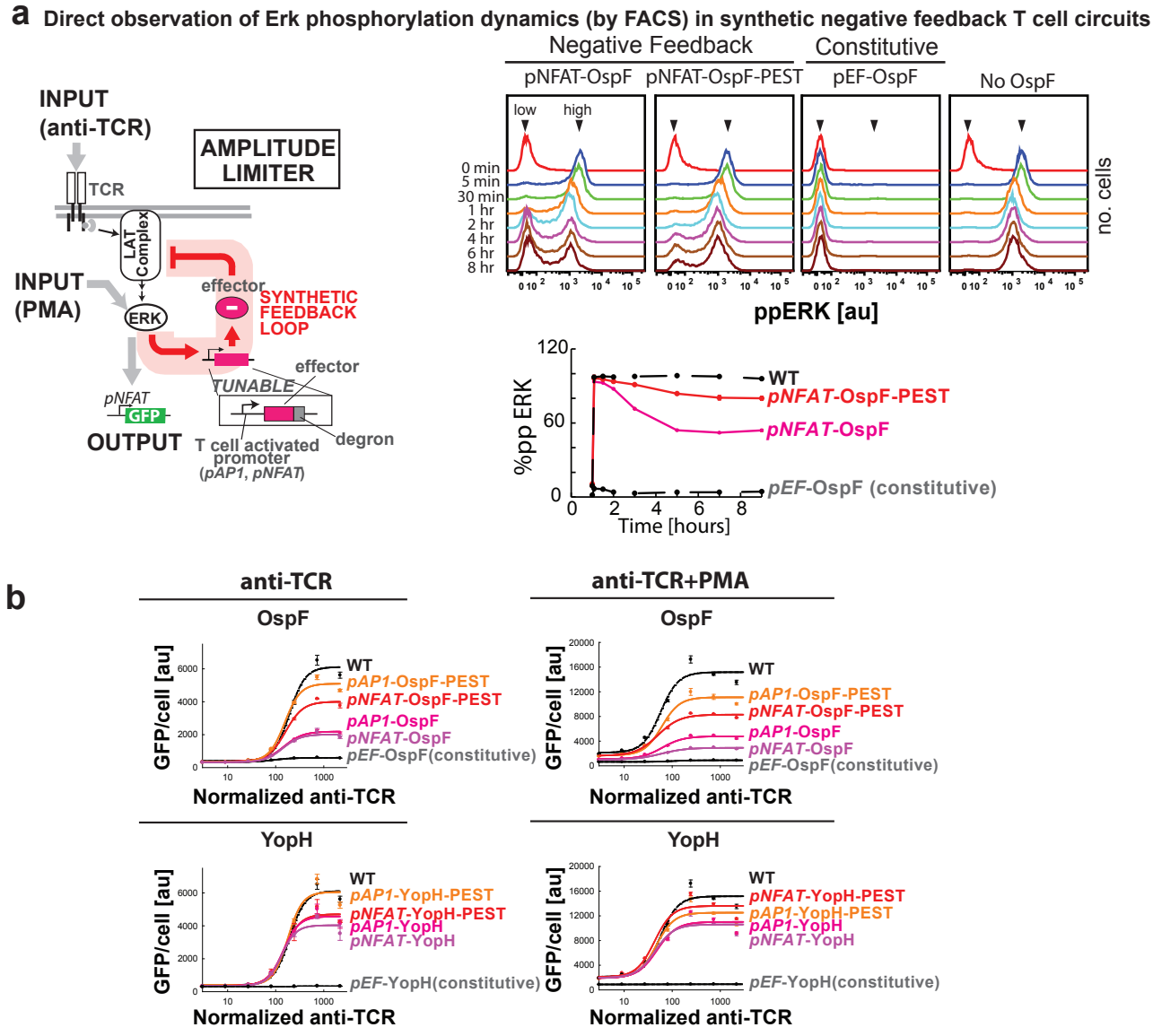

Supplementary Figure 7. Mechanism of amplitude limiter circuit: Introduction of OspF negative feedback loop causes transient Erk activation (instead of sustained), leading to lower steady pathway output amplitude. a, Histogram of the phospho-ERK at different time when stimulated with anti-TCR and PMA. PMA was used to sustain a normally transient pERK response, thus allowing the dynamics of negative feedback to be demonstrated. When OspF is expressed, a population of low pERK level appears. Constitutive expression of OspF has only low ppERK level while Jurkat without any OspF has only high of OspF population. With feedback loop, however, all cells displays high level of ppERK level after 5 minutes of activation, until after 1 hours of activation, when NFAT begins to express OspF and creat a population of low pERK cells. The percentage of active ERK as a function of time. (B) The dose response profile of NFAT transcription response for cells containing negative feedback loops built from YopH or OspF controlled by variant activity dependent promoters (*pNFAT, pAP1*), with or without the degron (*PEST*), induced by anti-TCR alone or anti-TCR supplemented with PMA. Constitutively expressed effectors (*pEF*) were used as negative controls.

Bacterial effectors can be engineered as pause switch to control T cell activation in Jurkat T cell

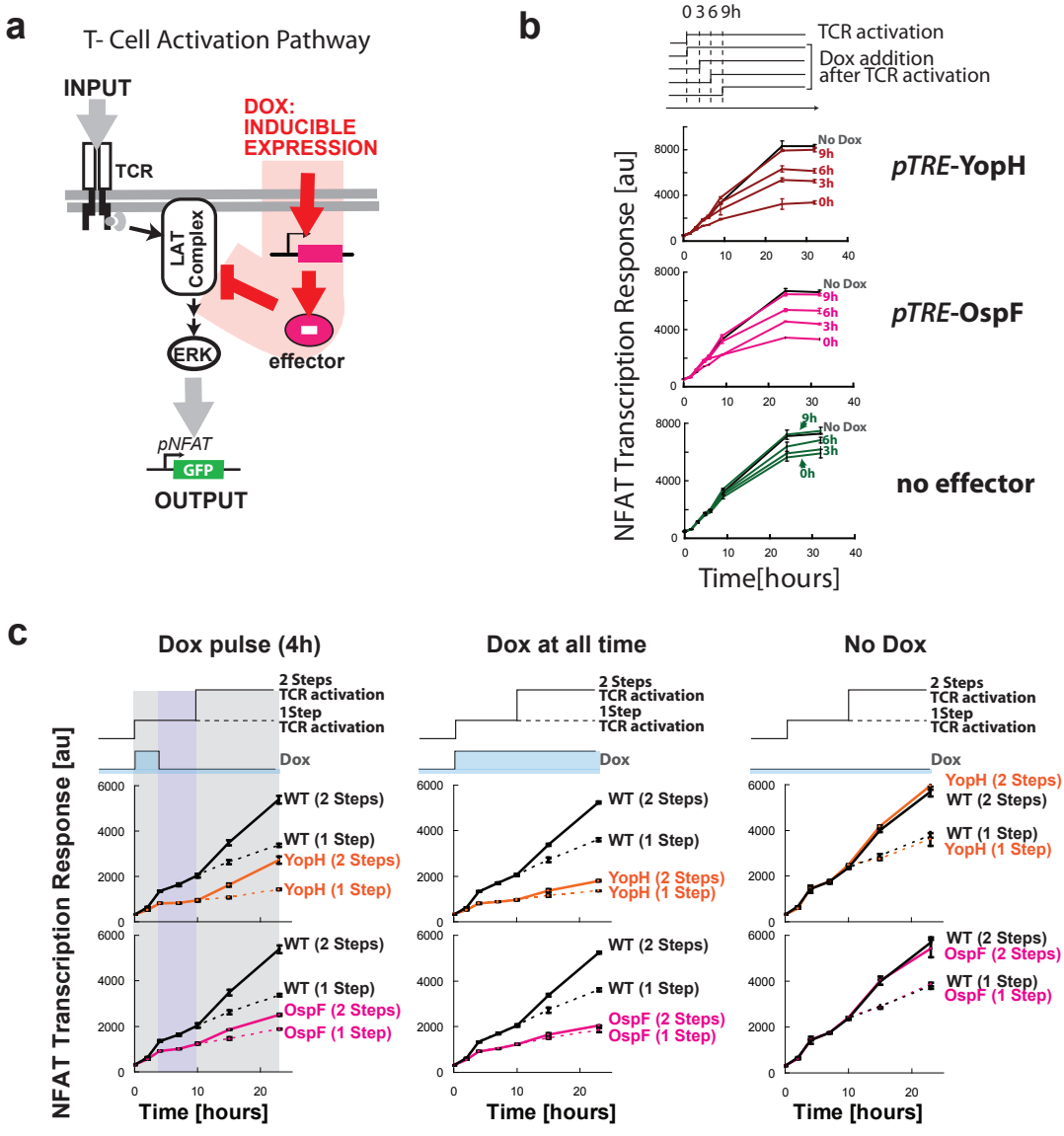

Supplementary Figure 8. Synthetic pause switch: Transient inhibition of TCR activation with a pulse induction of bacterial effectors. **a,** Using a tetracycline inducible promoter (*pTRE*), the expression of YopH and OspF can be controlled by the addition of doxycycline (dox). **b,** Dox induced expression of YopH and OspF at various time points after TCR activation. **c,** TCR is activated along with the addition of dox. In the left, after 4 hours, the cells were washed away of dox and incubate for 6hours before the TCR is further stimulated (solid line) or unstimulated (dash line). In the middle, TCR is activated along with the addition of dox, but without dox removal. In the right TCR is activated without any dox addition.

OspF can be used as a synthetic pause switch to inhibit the activation of human primary CD4+ T cells

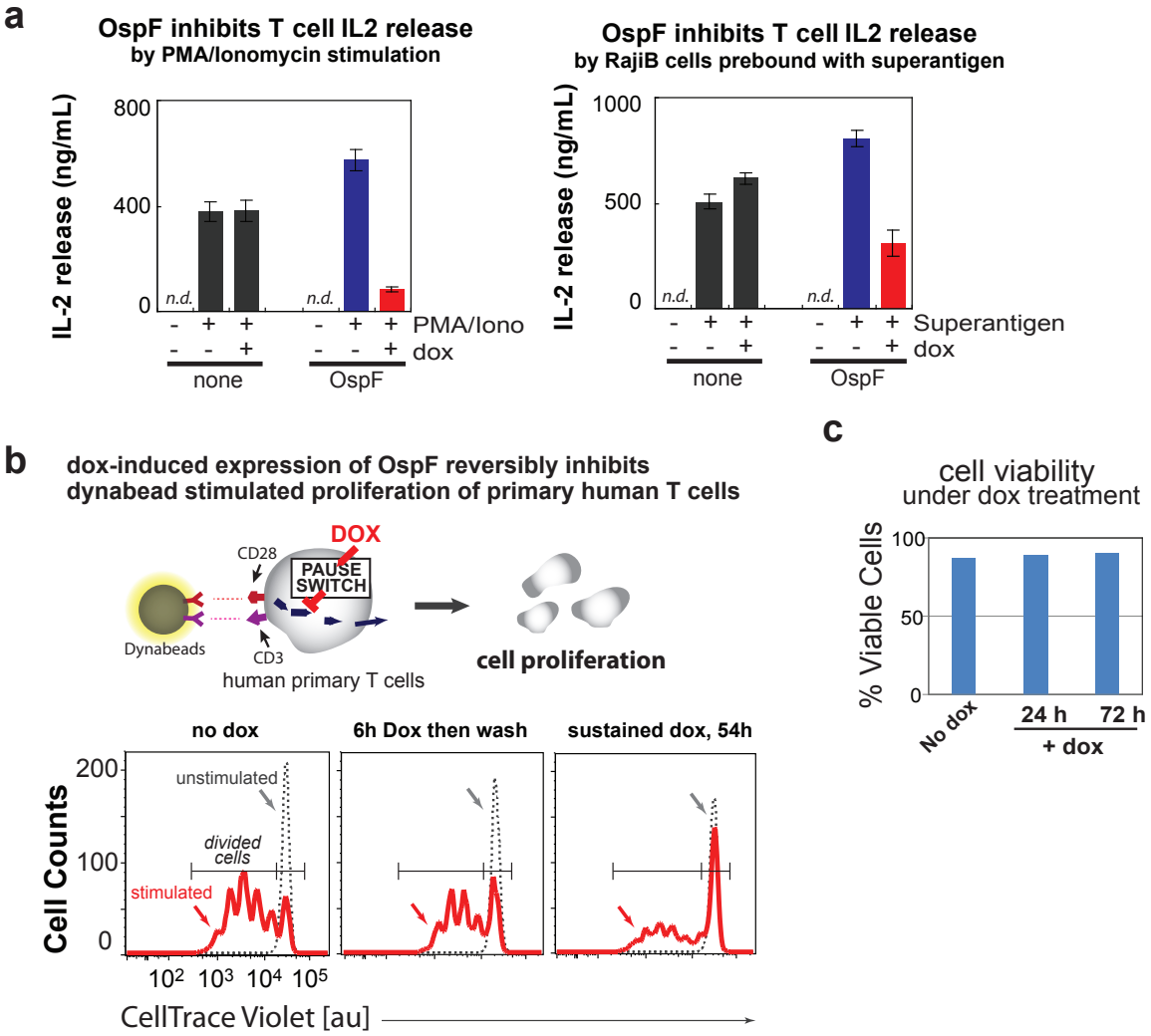

Supplementary Figure 9. OspF was engineered into a synthetic pause switch to control the activation of primary human T cells. a,The control T cells and T cells with OspF pause switch were pre-treated with or without 200ng/ml doxycycline for 6 hours and then activated with 10ng/ml PMA+0.5 mM ionomycine or Raji B cells pre-bound with superantigen peptides (1:1 ratio). IL-2 release was measured after 24 hours activation. **b,** The cells with OspF synthetic pause switch were treated without (left), with 6 hours (middle) or sustained dox (54 hours total) (right) were activated with anti-CD3 and anti-CD28 dynabeads (0.3:1 beads/cells ratio) for 4 days. Cells were labled with CellTrace violet dye before beads activation and measured with flow cytometry. The cells with low fluoresence density (red) indicated divided cells (diluted labeling dye in each single cell). The unstimulated cells with each dox-treatment did not proliferate (dot line, grey). **c,** The cell viability was measured after addition of 200ng/ml dox with live/dead cells dye. There is no evident of toxicity to human primary CD4+ T cells upon dox addition at 200ng/ml.